Aerodynamics of Drones with Auxetic Landing Gears During Perching Conditions

Magesh. M, Jawahar. P.K

Abstract*: This research investigates a quad copter that acts as a contactor of the perching process of birds with its auxetic graspers on the cylindrical surfaces. The perching system generates a time of yaw when a pitch / rolling control input during the drone landing is introduced by two different circumstances (high and forward flight). While in all situations the aggregate need for revolution every minute, pitch and energy consumption vs. flight vs, the auxetic environment enhances drone resistance in the treatment for spontaneous vibration talking. The suggested method stabilises frequency, yawing and rotating period with respect to the variable rate during perching.

***Keywords* : About four key words or phrases in alphabetical order, separated by commas.**

I. INTRODUCTION

Multirotor aircraft have increased in recent years as a base for small drones in applications ranging from monitoring, videography and delivery of items. The push-and-down times needed by the controlled airplane are produced by several different rotations per minute instead of by a large primary turbines with film and linear pitch output. Because of their simplicity and usability, they have become popular among hobbyists and scientists. In applications such as law enforcement, border and home security as well as surveillance, as well as company participation for apps such as package delivery or aerial photography, multi-rotor drones have shown interest. The quadcopter is the simplest to fly multi-rotor airplane with four rotors, normally built in a triangular frame and connected by boom with the fuselage. Two increasing riding strategies are possible on a quad. The first is a "plus" configuration with a certain shaft of the aircraft (Figure 1a). The second is the "passage" where two rotors direct the aircraft (Fig. 1b). Both types of aviation quadcopters have been considered in previous research. For the 2002 series of articles Pounds and Mahony et al. built and designed an cross-section quad-copter[1–4].. A quad-copter designed by Haviland et al. also concentrated on the link setup[5]. An intersecting Quadcopter was tested by Avera et al. in 2016 for use in the most populated metropolis. Extensive use was also found in the quadcopter plus setup. Stanford Multi-Agent II Autonomous Rotorcraft was built at Stanford University[7,8] and is a more configurable quadcopter. Two companies, Bouabdallah and Seigwart[9] and Erginer and Altuğ[10], have designed and built quad copters for more configurations. In 2011 Hrishikeshavan et al. noted the impact of hovers and edgewiss flows on the outcomes of microcopters with both plus and cap settings[11].]. More recently, Mueller and D'Andrea have developed a quad copter console with additional configurations for rotor energy failure [12]. Mulgaonkar et al. generated a quad-copter swarm [13] in the training plane plus configuration. Drone's skill was perfect in civil and military applications due to its excellent features like small aircraft sizes, simplicity of operation, various operations, vertical flight and docking, etc. [14]. The aircraft were extremely low in height and speed at launch and at dockage and limited command capacities [15]. If an airplane is starting harder it should be checked before the following flight [17] for harm, which takes a lot of time. A flexible aviation equipment can solve the problem. There are several research groups that have taken steps to build specialized landing gears. As shown in figure 1, the DARPA mission adaptive rotor (MAR) program includes a new autonomous car storage equipment made up of four robot weapons, modifying its position to keep the helicopter on track [18]. The helicopter stays stable and reduces the risk of the propeller hitting the pier.

II. MATERIALS AND METHODS

A. Real-Time Parameter Estimation

As stated above, the objective of parameter estimation growth is to produce an integrated methodology on microcontrollers that can still be calculated precisely in real time. A Fourier recursive transform in conjunction with a smaller approximation is therefore used to calculate the real time variable illustrated in this report. The resulting technique for the recognition of frequency-domain-systems provides useful input filters and a significant calculation and store effectiveness. Within a frequency area, an estimate of the model-based linear regression parameter must be formulated, but depending its dependent variable (angular acceleration). The velocity of a spinning detector is a horizontal change of six scales, the lowest quadratic pattern line for the direction of the corner. The current trend pitch is the angular speed, whereby it is estimated by the angular speed. q Is actually I − 5 maximum gyro detector rotation speed. Step q in seconds at the time of Tq's. Figure.1 it shows the time domains derivative

Revised Manuscript Received on December 16, 2019.
***** Correspondence Author
Magesh. M*, Assistant Professor, Department of Aerospace Engineering, B S Abdur Rahman Crescent Institute of Science and Technology, Chennai, India.
Jawahar. P.K, Professor, Department of Electronics and Instrumentation Engineering, B S Abdur Rahman Crescent Institute of Science and Technology, Chennai, India.

must however be correlated with the effects of the frequency domain approximation for the batch processing of the time domain.

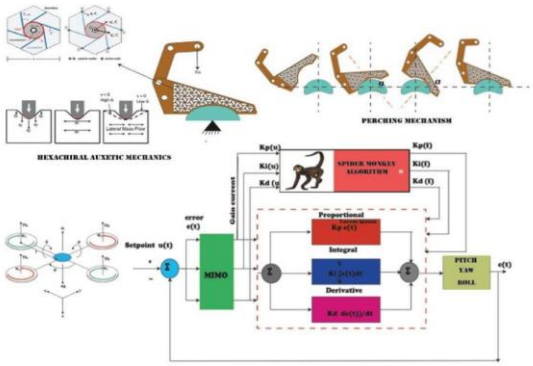

Fig. 1.Architecture of the proposed drone system

B. Hardware and Testing Methodology

With frame diameter (including batteries), a quadrotor of 0.45 m and a weight of 1.2 kg (2.64 lb) were constructed. Internal Microcontrollers can be used to monitor and transmit information to a laptop (X-Monkey, Ryan Mechatronics LLC). On-board measurements were made of a 3-axis, 3-axis barometrical altimeter, a 3-axis magnetometer, GPS and SD-deck. SD card management. Processors of 512 KB of flash memory, six KB of RAM, and five A-D outputs are the ARM LPC1768. ARM LPC1768 is given for the cpu. A non-linear flow reversal (NDI) aircraft machine was used for kinetic stabilization (see Alabsi and Fields for a detailed aircraft design explanation). All flight activities were manually operated and only used to stabilize the NDI command aircraft. To two-way information transmission to the office machine, a handheld cable modem (XBee, Digi Inc.) was used. Both state forecasts and checks were rendered at 100 Hz and 100 Hz was registered on the SD card. Because of the limited computing capability of microcomputers control and capture were not combined equally. Particularly in the SD card registration process, there are periodic breaks. Data are thus not distributed uniformly, so that further mistakes in the parameter estimation methodology will arise. There are roughly two percent variations between unevenly distributed FTR estimates and interpolated moment (the correct distance) in post-processing aircraft tests. The correlation of multisine outputs is predicted to be around 0.01 at standardized sampling intervals.

It is anticipated that torque and hydropower response torques will be directly in line with the Pn engine output (PWM output 0 to 1000 pulse). Submit commands to electronic speed control and task data lags will be transferred electronically into the folder. The entry period of multisine / drop is seen as part of the full Pn engine in the text, for convenience. The F engine, Rn stabilizer and multi-sine excitation signals are included each input order. The aim of the MSM is to encourage consistency so that documents have sufficient information to achieve high results in the simulation of accuracy. A number of four multi-axis models were developed wherein during single-axis pitch tests or spin experiments, only two sensors were enabled or all four were activated during single axis lag tests. Each multisine feed contained seven distinctive sinusoids. Table 2 gives full frequency and phase angle transmissions. The excitation time is 10 s for each multisine signal. Multi-sine performance amplitude control is important for information product accuracy. The tuning was conducted consistently in both solo and free flight tests, based on the reference signal / noise (SNR) ratio. The SNR can be used with a SNR of as low as 3. SNR over 3 does not imply reliable parameter estimation. An alternative quantitative simulation parameter called R2 is the proportion of the real performance variance expressed by the model in order to measure modeling accuracy. R2 is a given distance. R2 Tests utilizing different multisine amplitudes and test conditions have been performed with or without effective system control in a single axis rotational motion. Nominal experiments were carried out on completely intact propellers whereas a rotor injury test was conducted on a rotor with a damaged propeller maintaining 50% of the original length. An effective control scheme experiment enables the measurement of angle disruptions induced, energy gain ratio, input pair control and SNR inputs with adjustable input multisine amplitudes. The ability of parameter estimation technologies to correctly quantify certain motor / propeller efficiencies was assessed during the open-loop assessment of both input models using the model determination ratio. The Multisine A=4% rate, with no effective SNR power system after evaluating one-axis rotation motion, is adopted for F=50 percent maximum input over a period from 30s (Rn=0 for n=1;2;3... 4). This experiment almost continuously oscillates the quadcopter image, while information center 10s has been selected to evaluate parameters so that spontaneous behavior is not allowed. Initial ten s were missed to provide the parameter estimation algorithm with a static environment and to ensure that time changes in Parameter estimations were not caused by transient dynamics. The multisine wave amplitude has been selected with a minimum of 20 per cent, the lowest level for the stability of oscillatory yaws during the Yaw test, based on the SSR yield. Both engines have been given a continuing F 20 percent order. In all cases, compared to the rotor status and the lot estimates, results are calculated using the least time square in comparison with the estimated FTR (nominal in comparison with the damaged). Thanks to approximately the same effects for turn and spin movement, only spin movement results are given. Free flights were evaluated at the 750 ft2 University of Missouri-Kansas in the Drone Research and Teaching Laboratory (DRAT). In the DRAT laboratory, a quantity for safety net aircraft (12.1 to 8.2 meters / 9.2 ft) was developed, measuring 3.7 to 2.5 metres. Thanks to the mediated mountain-side distortion system during closed loop identification, the tests of distinct multisine amplitudes of A, 4 and 6 folden as shown in Table 4. Nominal checking with untouched engines was performed while there was a modified thrust which maintained the initial size of a certain engine 75 per cent during turbine impact test, as a broken 50%

propeller couldn't float securely with the car equipment and balance it with the engine equipment. The first 50s aircry was added to rolls and pitch axes and a period of about 80 seconds for the first 50s before the multi-pitch signal operation. For parameter estimates the center 10 s of the aviation data has been chosen. Both measurements are the same as the rotation of the single axis. The architecture of the system is a principal parameter that influences computational performance. During freeflight tests in literature, models presented are frequently used in which bonds were ignored. For two rolling system constructions, the residual from the observed contribution to the predicted results was plotted at open flow on the combination of term integration effect to the projected template accuracy and without the relation phrase. Depending on the presence of the sequence the remaining parts are examined. R2 has also been tested for both types with the same aircraft details.Figure.2it shows the If R2 increases by at least 0.5 million, the use of an additional development word in this circumstance is necessary.

Fig. 2.Photographic view of the experimental work

III. RESULT AND DISCUSSION

a. Hover

Each pole in Figure 3 is equivalent to the rigid-body method of the aircraft. The initial caps are four simple combined, three of which correspond to and modelled (surface effect and atmospheric change) the condition of the aircraft, which has no influence on their behavior. It's also zero on the dynamics of the aircraft. On the current line are four wheels in a hover that, next to the integraters, are all balanced. Such techniques are classified as hard, yeast, lowering of pitch and lowering of turn. If the quad-copter's vertical velocity is altered (e.g. upwards), more downwash on rotors increases the load contributing to a maximum lifting decrease. Since the aircraft started in a cutting state, this creates a downward acceleration. If the plane is down, the upwash boosts the rotor power, creating upward acceleration. Therefore, this process is moistened well. Secondly, if the speed of the aerial lake is disrupted, each rotor begins to travel in the plane. Aerodynamic strength works on each propeller and generates a net thrust against lake disruption (Fig. 19). The two main methods involve pitch and roller subsidies. The aircraft's nose up, front speed and nosedown pitch frequency are disturbed by pitch subsidence mode. The nose-down action contributes to a slower rate while the nose-down pitch frequency. When the plane turns, the rotor steps induced by an increase in the front rotors and a decline in the back rotors caused the plane to settle and limit nose-up acceleration. Likewise, spin, speed and lateral rate are part of the roll subsidy. The spin replacement process is operated the same as the slot alternative method, and the quadcopter invariantly runs in flora on both ends. The two forms of complex conjugated surfaces are a linear model and a horizontal phug style based on individual vector analysis. The transverse phugoid phase begins with a nosedown location (Fig. 2,). This is how the plane continues to continue. Aircraft nose path is initiated by aerodynamic pitch point linked to the longitudinal thrust assignment on each rotor and gravitable restoration cycles. When the pitch of the aircraft is positive (nose-up) and slows down the aircraft the rotor thrust reverses the path of transportation. The transmitting component from the forward portion is visually isolated, so that the sound variations between both parts are shown only for simpler reasons. It results in a peak noseup, reverting elements 6–8 and returning to element 1. A side phugoid treatment is also usable, replacing sideways with a forward moving pitch.

The Phugoid software involves the variants X SER, X MU and Sem, and MQ of the longitudinal stability. Through splitting the moment from front movement, the motor assignment and the resulting nose-up pitch period are established. In this case, the peak pitch angle at position 5 without other power is higher than at position 1, then the angle of pitch would be much higher if it was moved home to position 1. The system at this stage is therefore interrupted. Like with pitch drift, the frontrotor(s) is forced upwards in the atmosphere as the airplane travels upwards towards chin. The result is an additional inflow throughout the entire rotor, thus reducing the thrust. There a rotor(s) are also pressed down to increase the thrust. The rotors generate, taken together, a pitching moment. On the other hand, when the plane bats nosedown, a rolling point is made. Mq then seems to reinforce the framework and is a damping term. M is a kicking time that causes gravity that has an effect on a recovery moment and functions as phugoidal rigidity compared to a pitch speed. The lower the gravity centre, the safer the setting. The word Xu is a stream of the phugoid stabilizing expression. The composite force that works along the linear core leads to connections between rotational and space translations, shown by the change in aircraft form. Additionally, Y f, Yv, L μ, Lv and Lp are used in Lateral Phugoid Mode. The A flover entry as illustrated in Tab. 2 is a lateral moment or power equivalent ; e.g.: Y μm=-X S, Yv= XU, L¨=M S, L¨=M SS, Lv=-Mu and Lp μm2, minus Zw and Nr.. A north-eastern process representation contributes to sign shifts. The pole positions in plus and cross are precisely the same that the drone is supposed to rotate invariantly.

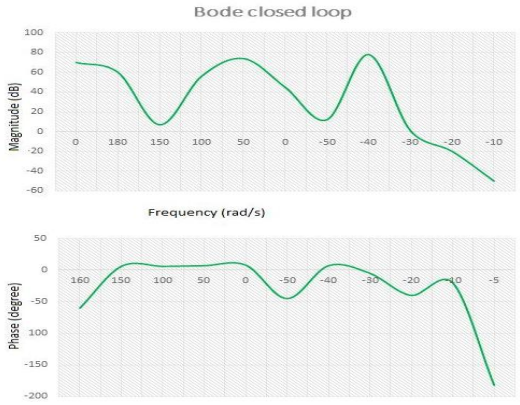

Fig. 3.Phugoid mode and augmented mode

b. Forward Flight

In the forward movement, the two phugoid strategies vary and become two distinct types of separate, distinct meanings. Usually, the longitudinal mode damping ratio improves at forward speed. Usually the directional phugoid procedure is flat until significant damping increases and at an elevated speed. Figure.4 it shows the average density of the longitudinal phugoid pattern is decreased to a peak of 7 m. The horizontal movement frequency rises to 9 m, with a reduction in theme. The side phugoid method is highly comparable in shape and is only combined with rolling position and rolling speed in lateral conversion. However, changes of altitude in longitudinal phugoid mode are included in the forward plane. This increases with the movement of the aircraft and sinks withdrawing. Pitch and roll subsidence points and hard elements of the forward-speed travel Figure.5. Illustration. The forward plane includes a common pitch and roll subsidy form, with a more robust roll subsidy at speed and less reliable pitch subsidies. At the same moment, the high model becomes more robust.Figure.6 it shows At an oscillatory short-term velocity of around 2.1 m the nodes linked to pitches and hard situations coalesce. In a foreflow of 9,1 m is divided into a pitch subsidence and a height of the complicated conjugate caps related to the short-run phase. It's a very damp method. The design of the plane at any level does not affect the quad copter's polar sites. Therefore, under all constant aerial conditions both plus and cross-configuration quad copter have highly comparable autonomous air dynamics.

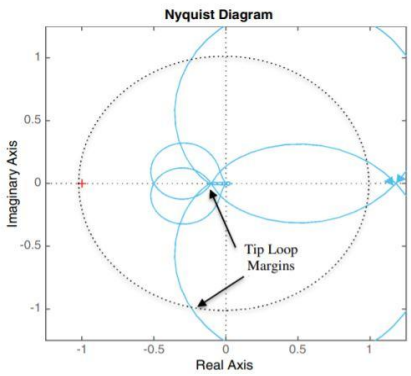

Fig. 4.Nyquist plot of the drone balance

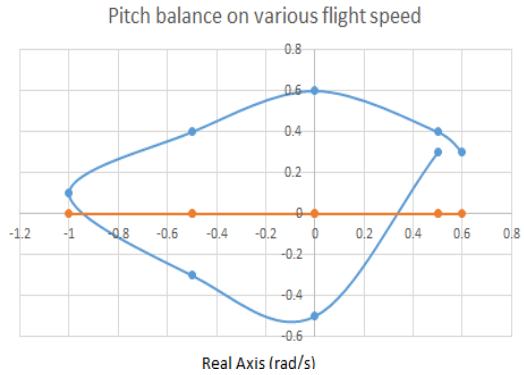

Fig. 5.Pitch balance on various flight speeds

The design of the plane at any level does not affect the quad copter's polar sites. Therefore, under all constant aerial conditions both plus and cross-configuration quad copter have highly comparable autonomous air dynamics Figure 6 and Figure 7 it shows the dampling ratio on various flight speeds and dampling ratio and natural frequency on forward speed.

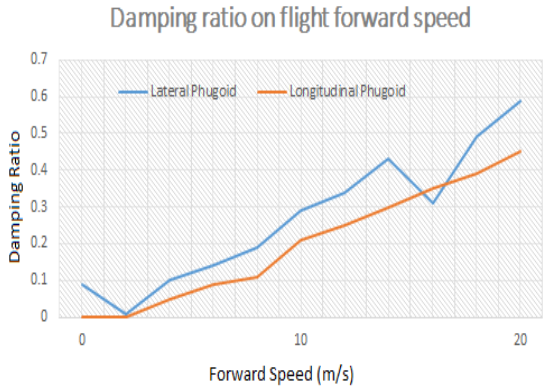

Fig. 6.Dampling ratio on various flight speeds

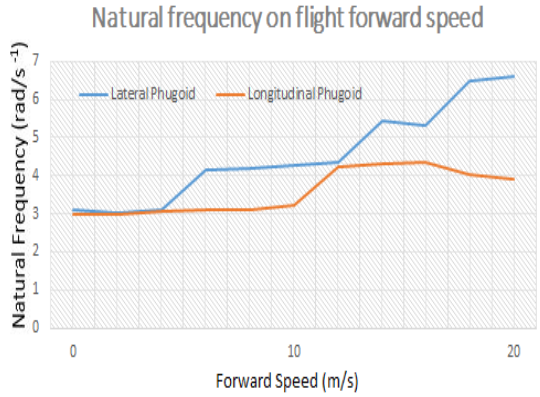

Fig. 7.Damping ratio and natural frequency on flight forward speed

This increases with the movement of the aircraft and sinks withdrawing. Pitch and roll subsidence points and hard elements of the forward-speed trav.Figure.8 and Figure.9 it shows the Torgue for various angular velocity and thurst for angular velocity.

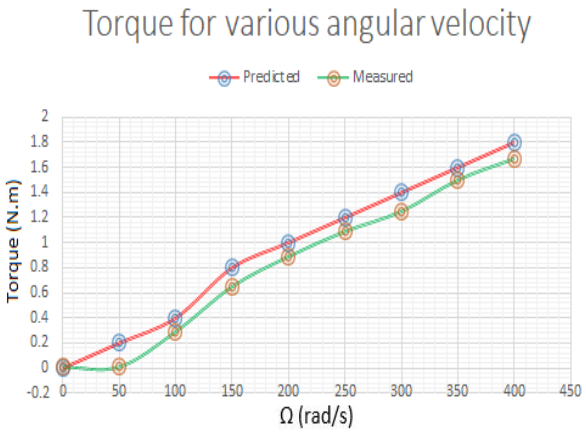

Fig. 8.Torque for various angular velocity

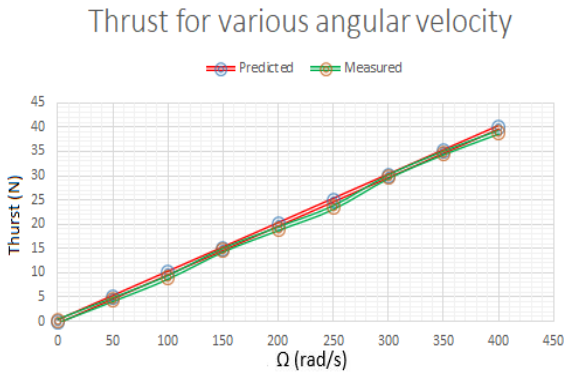

Fig. 9.Thrust for various angular velocity

ACKNOWLEDGMENT

Our sincere thanks to *Mr.R.Raj Jawahar* for providing technical support to conduct the proposed research work under his guidance.

IV. CONCLUSION

This paper contrasts a quad copter in plus and bar environments. Each setup is connected to various rotor controls with collective cycle per minute, pitch, spin and layer control. The input of pitch and spin is Yaw moment; for cross-configuration, the pitch and roll command is isolated from Yaw. The quad copter is designed as a static structure with six liberty groups which track variables of movement, taking the balance of power and time of three components into consideration. Three to four (10-status) peters models also measure the respective turbine pressures using the main component concept in terms of core resistance and gravitational consequences. A linear design is developed to check aviation mechanics autonomously by constantly condensing the floods and to lower the problem. The quad copter configuration of the 0–14 m / spin studios does not influence the speed of 0–14 m / collective phases. For a longer quad-copter the need for pitch regulation is greater than a shuttle unit, because four rotors produce pitch moment as compared to two for super-installation. A front-flight yaw controller is also required for the quad copter to settle down. An examination of autonomous flight dynamics revealed that in quad copter two models are displayed in the hover: transverse phugoid (coupled longitude and tilt) and side phugoid (coupled to rolled) mode. All methods are stable and have chance in their bases. Both methods are different in preparation and the duration and damping of both approaches are improved. The horizontal phugoid mode is very close to that of the forward one, but altitude adjustments begin with longitudinal phugoid mode (in addition to horizontal pitching and conversion).. In order to arrive at a quick-term method of oscillation, multiple real poles (relevant to heavy and pitcher subside) collapse over a certain airspeed distance. For individual vivid features (pole location) there are no important changes between plus and cross environments. A contrast between the control capacity available for the multi-and the multi-configuration quads indicates that the individual and yacht control functionaries are identical, but the pitch-flow control functionaries are up to 2 pp times larger for cross-configuration, as all 4 rotors are being used (unlike only 2 for plus).

REFERENCES

1. P. Pounds, R. Mahony, P. Hynes, J. Roberts, "Design of a FourRotor Aerial Robot," *In Proceedings Australasian Conference on Robotics and Automation* ,2002, pp.145-150.
2. P. Pounds, R. Mahony, P. Hynes, J. Gresham, J. Roberts, "Towards Dynamically Favourable Quad-Rotor Aerial Robots", In *Proceedings of the 2004 Australasian Conference on Robotics & Automation*, 2004.
3. P. Pounds, R. Mahony, P. Corke, J. Roberts,"Modelling and Control of a Quad-Rotor Robot*", In Proceedings Australasian Conference on Robotics and Automation*, Dec. 2006.
4. P. Pounds and R. Mahony., "Design Principles of Large Quadrotors for Practical Applications," *In International Conference on Robotics and Automation*, May. 2009, pp. 3265–3270
5. S. Haviland, D. Bershadsky, D. Magree and E. Johnson, "Development of a 500 Gram Vision-based Autonomous Quadrotor Vehicle Capable of Indoor Navigation," 71st Annual Forum of the American Helicopter Society International, American Helicopter Soc. Paper 248, Virginia Beach, VA, May 2015.
6. M. Avera, M. Kand, R. Singh, "Performance and Controllability Assessment of an Overlapping Quad-Rotor Concept," *In 72nd Annual Forum of the American Helicopter Society International*.,May 2016, Paper 14.
7. G. Hoffmann, H. Huang, S. Waslander, C.Tomlin, "Quadrotor Flight Dynamics and Control: Theory and Experiment *In AIAA guidance, navigation and control conference and exhibit*,Agu. 2007, pp.6461.
8. H. Huang, G. Hoffmann, S. Waslander, C. Tomlin, "Aerodynamics and Control of Autonomous Quadrotor Helicopters in Aggressive Maneuvering," *2009 IEEE International Conference on Robotics and Automation*, May 2009, pp. 3277–3282.
9. S. Bouabdallah, R. Seigwart, "Full Control of a Quadrotor," *International Conference on Intelligent Robots and Systems*, Oct. 2007, pp. 153–158.
10. B. Erginer, E. Altuğ, "Modeling and PD Control of a Quadrotor VTOL Vehicle," *Intelligent Vehicles Symposium*, Jun.2007, pp. 894–899.
11. V. Hrishikeshavan, J. Black, I. Chopra, "Development of a Quad Shrouded Rotor Micro Air Vehical and Performance Evaluation in Edgewise Flow," *In Proceedings of the American Helicopter Society Forum*, May 2012.
12. M. Mueller, R. D.'Andrea, "Stability and Control of a Quadrocopter Despite the Complete Loss of One, Two, or Three Propellers," *International Conference on Robotics and Automation*, May. 2014, pp. 45–52.
13. Y. Mulgaonkar, G. Cross, V. Kumar, "Design of Small, Safe, and Robust Quadrotor Swarms," *International Conference on Robotics and*

Automation, May .2015, pp. 2208–2215.
14. C. P.Jiang, "Research on Design and Realization of Control System for a Quadrotor Unmanned Aerial Vehicle", *Harbin Institute of Technology*, 2014.
15. S. L.Wang. "Research on Design Technology of Automatic Take-off and Landing for UAV", *Nanjing University of Aeronautics and Astronautics*,2011.
16. Vasudevan Manivannan, P. Jared ,F. Langley Mark Costello,Massimo Ruzzene, "Rotorcraft Slope Landings with Articulated Landing Gear", *Georgia Institute of Technology, Atlanta*, 2013.
17. J. Kiefer; M. Ward; M. Costello. "Rotorcraft Hard Landing Mitigation Using Robotic Landing Gear",*Journal of Dynamic Systems, Measurement, and Control*, 138(3),Mar.2016, p.031003.
18. Daniel Melia Boix; Keng Goh; James McWhinnie,"Modelling and Control of Helicopter Robotic Landing Gear for Uneven Ground Conditions", *In Workshop on Research, Education and Development of Unmanned Aerial Systems* ,Oct.2017,pp.60-65.
19. W.-K. Chen, *Linear Networks and Systems* (Book style). Belmont, CA: Wadsworth, 1993, pp. 123–135.
20. H. Poor, *An Introduction to Signal Detection and Estimation*. New York: Springer-Verlag, 1985, ch. 4.
21. B. Smith, "An approach to graphs of linear forms (Unpublished work style)," unpublished.
22. E. H. Miller, "A note on reflector arrays (Periodical style—Accepted for publication)," *IEEE Trans. Antennas Propagat.*, to be published.
23. J. Wang, "Fundamentals of erbium-doped fiber amplifiers arrays (Periodical style—Submitted for publication)," *IEEE J. Quantum Electron.*, submitted for publication.
24. C. J. Kaufman, Rocky Mountain Research Lab., Boulder, CO, private communication, May 1995.
25. Y. Yorozu, M. Hirano, K. Oka, and Y. Tagawa, "Electron spectroscopy studies on magneto-optical media and plastic substrate interfaces(Translation Journals style)," *IEEE Transl. J. Magn.Jpn.*, vol. 2, Aug. 1987, pp. 740–741 [*Dig. 9th Annu. Conf. Magnetics* Japan, 1982, p. 301].
26. M. Young, *The Techincal Writers Handbook.* Mill Valley, CA: University Science, 1989.
27. (Basic Book/Monograph Online Sources) J. K. Author. (year, month, day). *Title* (edition) [Type of medium]. Volume(issue). Available: http://www.(URL)
28. J. Jones. (1991, May 10). Networks (2nd ed.) [Online]. Available: http://www.atm.com
29. (Journal Online Sources style) K. Author. (year, month). Title. *Journal* [Type of medium]. Volume(issue), paging if given. Available: http://www.(URL)

AUTHORS PROFILE

Magesh Mani received the B.E. degree in electronics and electronics engineering from the Anna university, India, in 2005, the M.E. degree in Avionics from Madras Institute of technology, Anna University, India, in 2007. He has 09 years of teaching experiences and 03 years of Industrial experiences, he is currently a Assistant Professor with the Department of Aerospace Engineering, B.S.A. Crescent Institute of Science and Technology, Chennai. His current research interests include Navigation system, UAV/MAV Design, guidance and control, and autopilot.

Periyan Kandasamy Jawahar received the B.E. degree in electronics and communication engineering from the Coimbatore Institute of Technology, Coimbatore, India, in 1989, the M.Tech. degree in electronics and communication engineering from the Pondichery engineering College, Pondicherry, India, in 1998, and the Ph.D. degree in information and communication engineering from Anna University, Chennai, India, in 2010. He has 22 years of teaching experiences and he is currently a Professor with the Department of Electronics and Communication Engineering, B.S.A. Crescent Institute of Science and Technology, Chennai. His current research interests include wired and wireless networks, very large scale integration, microprocessor, and microstrip antenna.profile which contains their education details, their publications, research work, membership, achievements, with photo that will be maximum 200-400 words.